Neutron-scattering investigation of the phonons in intermediate-valence $Sm_{0.75}Y_{0.25}S$†

H. A. Mook and R. M. Nicklow
Solid State Division, Oak Ridge National Laboratory, Oak Ridge, Tennessee 37830
(Received 12 February 1979)

Neutron-scattering techniques have been used to measure the phonons in intermediate-valence $Sm_{0.75}Y_{0.25}S$. Anomalies are found in the shape of the phonon dispersion curves and in the phonon widths that are attributable to mixed-valence effects. Phonon positions and widths are shown as a function of temperature. The greatest phonon softening and the largest phonon widths are found at the valence transition that occurs at 200 K. A screened-rigid-ion model has been used to fit the phonon dispersion curves. The model reproduces the general shape of the phonon dispersion data but fails to account for the anomalies.

I. INTRODUCTION

There continues to be considerable interest in the mixed-valence state from both the theoretical and experimental viewpoint.[1,2] The physical properties of materials are obviously greatly affected by the valence state and even the lattice constant can be very dependent on valence changes in the material. One of the best known examples of this is SmS which has a lattice constant of about 5.97 Å when the Sm has a valence of 2 and a much smaller lattice constant, 5.70 Å, when the Sm is in a valence state intermediate between 2 and 3.[3] Since the lattice constant is such a strong function of the valence state, it is expected that phonons play an important role in materials with a fluctuating valence state. Phonon measurements on SmS in the mixed-valence state would have to be performed with high-pressure cells, and scattering and absorption by the pressure cell add considerably to the difficulty in performing neutron scattering measurements. One can avoid the necessity of high-pressure cells by alloying YS with SmS which produces a lattice collapse similar to that obtained with high-pressure experiments.[4] This results in an intermediate-valence material that can be studied at standard pressures. Preliminary results of phonon measurements on this material have been published in Ref. 5. This paper will show additional measurements on (Sm,Y)S and present detailed information on the dispersion curves and phonon widths as a function of temperature. We will also show the results obtained by fitting the phonon dispersion curves with a screened-rigid-ion model. Although the model roughly describes the data, it is obvious that a more sophisticated model that can take into account valence fluctuations is needed for a good description of the phonon data.

The neutron absorption of natural Sm makes neutron studies of Sm compounds impossible unless Sm is used which is highly enriched in one of the less absorbing isotopes. The best of these is ^{154}Sm, but the material is very expensive and only small amounts of it are available. Thus, while it would be more informative to perform experiments on a series of alloys of varying composition, we found that this would be impossible, and it was necessary to choose only one alloy composition. We chose the composition $Sm_{0.75}S_{0.25}Y$, and we used Sm enriched to 99% in ^{154}Sm. This composition shows a gradual valence change with temperature and thus we hoped that the crystals could be cycled through the valence transition without breaking. We were mostly successful in this regard; however, one of our largest crystals did break upon warming through the transition. The lattice constant versus temperature of our sample of $Sm_{0.75}Y_{0.25}S$ is shown in Fig. 1. At room temperature the material is gold in color and has a lattice constant of 5.695 Å. As the material is cooled, it expands and turns to a dark purple or black color. The lattice constant goes through a broad transition centered at about 200 K and levels off to a value of about 5.760 Å at low temperatures. More accurate lattice-constant measurements show that the lattice constant

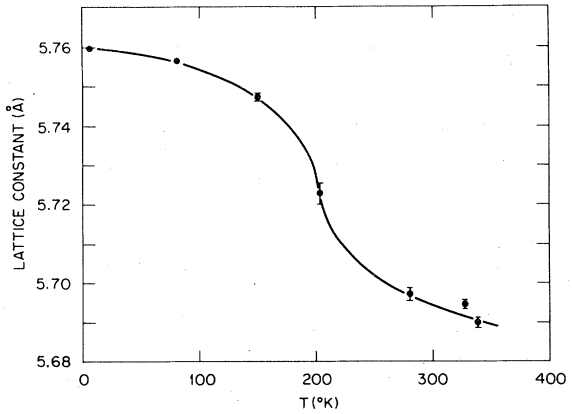

FIG. 1. Lattice constant vs temperature for $Sm_{0.75}Y_{0.25}S$.

is slightly smaller at 100 K than the value suggested in Ref. 5. The lattice constant is well defined at each temperature and no spread in lattice constant was observable with the standard spectrometer resolution using 0.4° mosaic spread graphite monochromator and analyzer crystals. High-accuracy lattice-constant measurements using perfect silicon crystals showed that the mosaic spread of the crystals increased somewhat (0.2°) at the transition at 200 K. However, this small increase in mosaic spread is far too small to affect the resolution of the phonon measurements. The neutron beam samples the entire crystal volume showing that the lattice constant is uniform through the whole sample. The valence state of the alloy can be estimated by interpolating between the lattice constant for $Sm^{2+}S$ (5.97 Å), $Sm^{3+}S$ (5.62 Å), and YS (5.50 Å). Using a linear interpolation results in a configuration that is 30% Sm^{2+} at 293 K, 50% Sm^{2+} at 200 K, and 70% Sm^{2+} at 10 K.

$Sm_{1-x}Y_xS$ solid solutions have been examined by x-ray photoemission,[6,7] and by the Mössbauer isomer shift.[8] These measurements show the intermediate-valence nature of the $Sm_{1-x}Y_xS$ system and there is reasonably good agreement between the Sm valence state obtained from these techniques and from lattice-constant interpolation. In addition, the isomer shift measurements show that the alloy system has a homogeneously mixed valence. The energy resolution of the x-ray photoemission and isomer shift measurements also introduce a time scale into the intermediate-valence problem. X-ray photoemission has very coarse resolution and thus a short sampling time, on the order of 10^{-15} sec. The photoemission results show both valence states existing simultaneously and thus imply that fluctuations between the valence states must be slower than 10^{-15} sec. The Mössbauer isomer shift measurements have very high resolution and a sampling time of around 10^{-9} sec. These measurements show one line at an intermediate valence so that the valence fluctuation time must be shorter than 10^{-9} sec. The magnetic excitations in $Sm_{0.75}Y_{0.25}S$ have been examined by neutron-diffraction techniques.[9] It is found that the 7_{F_0}-7_{F_1} transition for the Sm^{2+} ion is broadened considerably in the intermediate-valence state. The broadening is about 15 meV suggesting a fluctuation time longer than 3×10^{-13} sec. The fluctuation rate thus appears to be comparable to the phonon frequencies and one might expect pronounced intermediate-valence effects to be visible in the phonon measurements.

II. PHONON MEASUREMENTS

The phonon measurements were made on crystals of $Sm_{0.75}Y_{0.25}S$ at the High Flux Isotope Reactor using the standard triple-axis neutron scattering technique. Singly bent pyrolitic graphite and flat pyrolitic graphite were used as the monochromator and analyzer crystals. The mosaic spread of both monochromator and analyzer was about 0.4°. Collimators of 0.66° were used before and after the sample. Collimation before the monochromator and after the analyzer was limited by geometry to about $1\frac{1}{2}$° and 3°, respectively. The analyzer energy was fixed at 3.563 THz, and the incident energy was varied in the experiment. A pyrolitic graphite filter was used to remove higher-order contaminations in the analyzer.

Five small single crystals were used in the measurements. The biggest of these was about 0.5 cm on a side. All acoustic-phonon measurements were made with one sample crystal at a time. The crystal was held in a holder by a small spring so that no strains would be introduced by a sample holder upon cooling or warming. Still one crystal broke upon warming during one of the earlier measurements. Fortunately, no breakage occurred in subsequent measurements on other crystals. The optical phonons were difficult to measure because of the small scattering amplitude of sulfur and because they were very broad in energy in some cases. Some of the optical-phonon measurements were made by stacking together four crystals giving a sample volume of slightly less than 0.5 cm^3. Since the sample crystals had flat faces aligned along (100), the crystals were easily aligned and the sample mosaic spread with the four crystals was under 1.5°. This mosaic spread had little effect on the optical-phonon measurements.

Figure 9 shows the phonon dispersion curves. The dispersion curves look similar to what one might expect to find for a standard rock-salt structured material having very small ionic charges. There are, however, anomalies in the dispersion curves and in the phonon widths which we feel are a direct result of valence fluctuations. The LA modes are soft compared to the TA modes especially for the [110] and [111] directions. The LO modes are soft also and fall below the TO for the three principal directions. We find that large phonon widths are associated with the soft-phonon branches. The unusual properties of the phonon dispersion are discussed in Ref. 5.

Figure 2 shows some constant-Q phonon scans made in the [111] direction. The acoustic phonons are fairly easy to measure except somewhat longer counting times are needed where the phonons are very broad in the region 0.35 of the way to the zone boundary in the [111] direction. We will henceforth adopt an abbreviated notation for reciprocal-space positions such that the above position will be denoted by $\xi\xi\xi = 0.35$. We feel that the broadening and softening of the LA[111] phonon is a result of valence fluctuations. This is supported by temperature-dependent measurements which show that the largest phonon softening and broadening takes place at the temperature of the valence transition which is about 200 K. The LA phonon in the

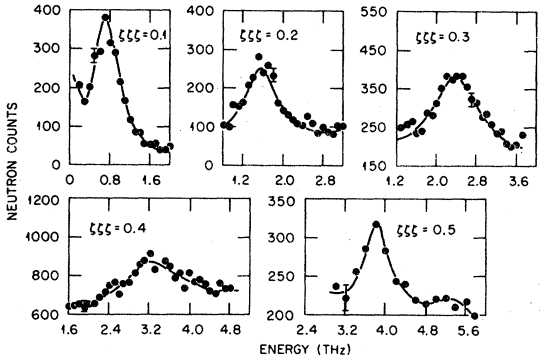

FIG. 2. Constant-Q scans of the LA branch for the [111] direction.

[110] direction is also soft compared to the transverse phonons and indeed lies lower in energy than the TA2 phonon over part of the zone. Ultrasonic measurements showed that soft LA phonons were expected at $q=0$ but, of course, provided no information on how far into the zone this softening would persist.[10]

Figure 3 shows the widths of the LA phonons measured in the [111] direction with the spectrometer resolution removed. The spectrometer resolution was calculated using standard techniques and experimentally checked in the vicinity of the Bragg reflections. The spectrometer resolution was about 0.3 THz over most of the zone reaching a maximum of about 0.6 THz at the zone boundary. We see that the phonon widths are very large about $\frac{2}{3}$ of the way to the zone boundary but are small at both $q=0$ and the zone boundary. The transverse phonons are narrow in all cases and show no unusual features. Figure 4 shows a comparison of the TA and LA phonons. While the LA phonon at $\xi\xi\xi=0.35$ is quite broad, the TA phonon width appears to be resolution limited. Very narrow TA phonons could be measured where good focusing was possible. The bottom graph in Fig. 4 shows a well-focused phonon for the [110] direction. The width is only 0.15 THz and is resolution limited. The fact that very narrow TA phonons can be measured shows the sample is of high quality. The widths of the TA phonons are sensitive to small changes in lattice parameter or mosaic spread. It seems that the TA phonons are not affected much by the valence fluctuations. This is to be expected since to first order the transverse phonons do not affect the volume of the unit cell. X-ray diffraction measurements of Debye-Waller factors by Dernier *et al.*[11] for $Sm_{0.7}Y_{0.35}$ have shown that the S displacements become anomalously large near the valence transition, and they have suggested that a softening of the optic phonons takes place at the transition. LO phonons do appear to be greatly affected particularly at the [111] zone boundary. However, the fluctuating valence state strongly affects the LA phonons as well particularly for the [111] direction.

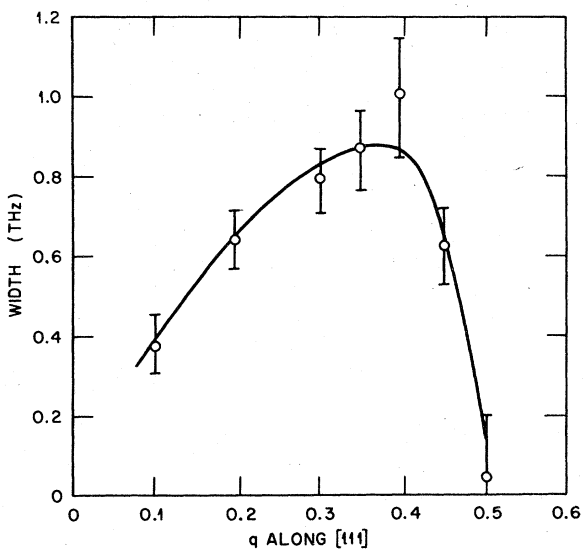

FIG. 3. Phonon widths for the [111] LA branch. The contribution to the widths from the spectrometer resolution has been removed from the data.

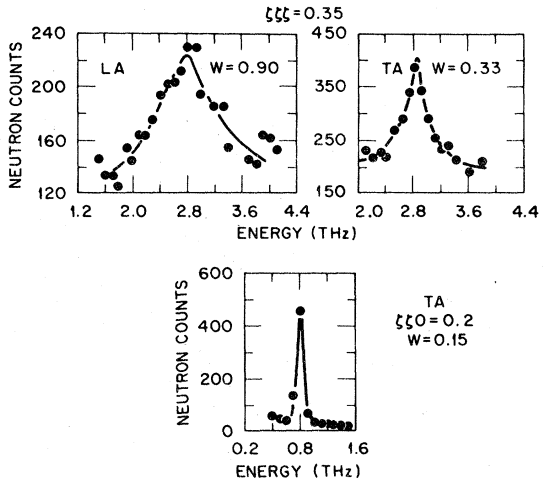

FIG. 4. Comparison between LA and TA phonons. The top two graphs show phonons measured 0.35 of the way to the zone boundary for the [111] direction. The bottom graph shows a well-focused TA phonon measured in the [110] direction. The width, w, is given in THz.

Figure 5 shows some of the optical-phonon measurements. These measurements were generally much more difficult than the acoustic-phonon measurements because of the low scattering amplitude for S, lower inelastic scattering structure factors, and the large widths of some of the phonons. The phonon measurements were easiest at the Γ point as is usually the case and generally hardest near the zone boundary. The width of the phonons measured at Γ were

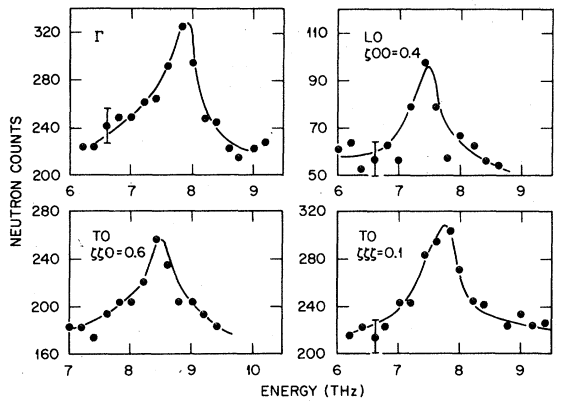

FIG. 5. Measurements of some optical phonons.

resolution limited as were all TO phonons within the error of measurements. It appears once again that the valence fluctuations do not strongly affect the transverse phonons. However, some of the LO phonons were very broad. The LO phonon at the [111] zone boundary is so broad that scattering can be seen all the way down to LA phonon. The center of the intensity distribution for this phonon appears to be at about 7 THz, but the phonon is sufficiently broad that it really is not a well-defined excitation. The [111] zone-boundary phonon obviously couples very strongly the valence fluctuations. This is in agreement with the x-ray determined Debye-Waller factor measurements[11] and with light scattering measurements of the optical-phonon frequencies in mixed-valent materials.[12]

III. TEMPERATURE-DEPENDENT MEASUREMENTS

Since the valence state of the $Sm_{0.75}Y_{0.25}S$ sample is a function of temperature the unusual phonon properties caused by valence fluctuations should be temperature dependent. There may be intrinsic phonon widths because of alloy effects; however these widths should not be strongly temperature dependent. We find that the phonon anomalies in $Sm_{0.75}Y_{0.25}S$ are strongly temperature dependent and are largest at the valence transition near 200 K. The top scans in Fig. 6 are measurements of the LA phonons for $\xi\xi\xi = 0.3$ for three temperatures. Both the phonon widths and positions are temperature dependent. The LA phonon dispersion curve for three temperatures is shown in Ref. 5. There are two temperature-dependent effects on the dispersion curve. At the lower values of q the phonon dispersion curve softens as the sample is cooled to the valence transition temperature and then increases in energy as the temperature is lowered further. At low temperatures the sample color is back and the valence is closest to the 2+ value. The phonon energies at low temperatures approach the value of the phonon energies for SmS

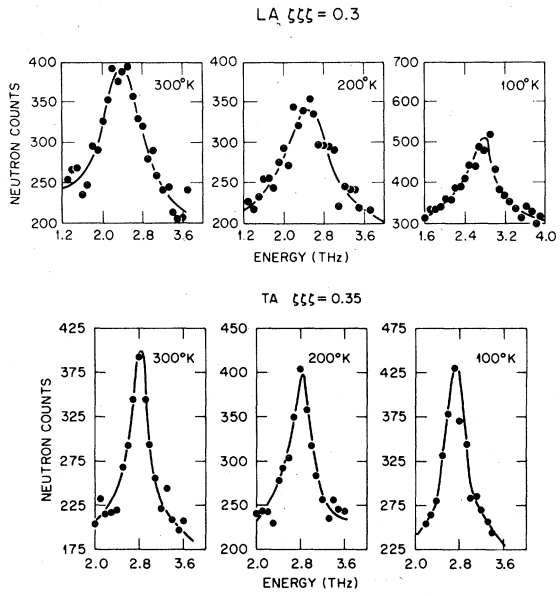

FIG. 6. Top three scans are LA phonon measurements for the [111] direction for three different temperatures. The bottom three scans are TA phonon measurements at the same three temperatures. Note the scale change for the LA phonon 100 K measurement.

which is completely in the 2+ state.[13] It seems clear that the phonon shift at low q is a result of the fluctuating valence since the maximum phonon softening occurs at the valence transition. Another temperature-dependent effect is that the zone-boundary energies increase continuously with decreasing temperature. This is the normal behavior expected for anharmonic effects. Also since the lattice constant of the sample is a continuous function of temperature, we expect some changes in the phonons as the sample unit cell changes size. Since the zone-boundary phonon energy changes continuously in the same direction with temperature, the change is probably not a mixed-valence effect, but the result of the continuous change in electronic properties as the sample is cooled. Figure 7 shows a plot of the phonon shifts as a function of temperature. We see that the phonon energies increase considerably at 100 K. For low q the phonon branch is softest at the valence transition at 200 K. However, as q increases toward the zone boundary, the minimum at the valence transition is removed by the strong upward zone-boundary shift of the dispersion curve upon cooling. Thus, at the valence transition there appear to be two competing effects. The strong valence fluctuations at 200 K tend to soften the phonon energies but the continuous changes in the electronic properties tend to increase the phonon energies particularly near the zone boundary. The lower scans in Fig. 6 are TA phonons at three temperatures for $\xi\xi\xi = 0.35$. These

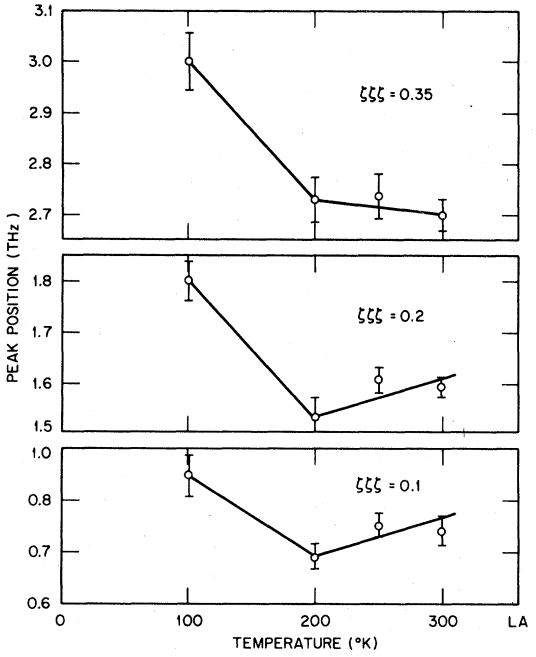

FIG. 7. Phonon energy shifts as a function of temperature for the LA [111] branch.

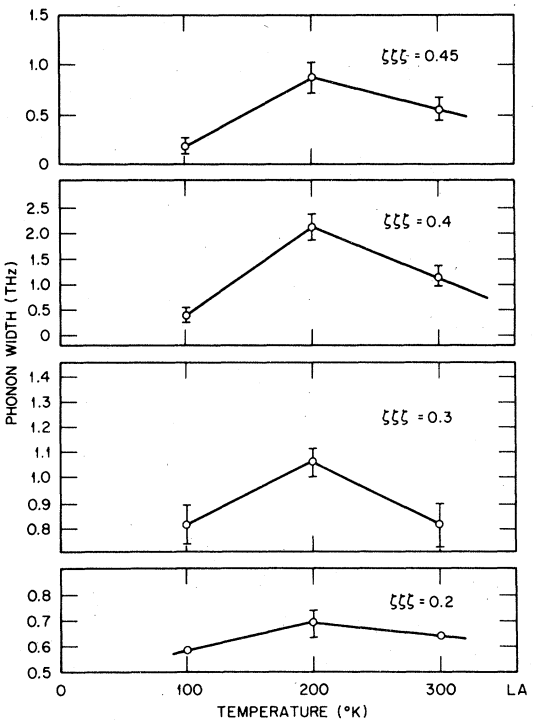

FIG. 8. LA phonon energy widths for the [111] direction for three temperatures.

phonons are narrow in all cases and temperature independent. Again we see the intermediate-valence effects are confined to the longitudinal phonons as expected. The [111] LA phonon energy increases so much at low temperatures that the very unusual feature of the LA branch falling below the TA branch disappears at low temperatures.

Figure 8 shows the temperature dependence of the phonon energy widths for the [111] LA branch. We see that the maximum width occurs at the valence transition in all cases. We feel that this is convincing evidence that the widths are a result of the valence fluctuations. Widths from alloy effects would not show this temperature dependence. Furthermore, the TA phonons show no intrinsic width whereas single-site mass-defect coherent-potential approximation (CPA) calculations would predict identical phonon widths for the TA and LA modes of the same energy for a random alloy. The very large phonon widths suggest strong coupling between the phonons and valence fluctuations and any theoretical calculations for phonons in mixed-valence materials must take the large widths into consideration.

Similar effects are found for the phonons propagating along the other principal directions although they are not as pronounced as for the [111] direction. Table I shows the elastic constants obtained from low-q phonon measurements for three temperatures. The bulk modulus B is also shown and we see the bulk modulus is smallest at the valence transition as we expect. In fact at low temperature where the material has its intermediate-valence value closest to integral valence the bulk modulus is about three times the value at the transition.

A few measurements of the optical modes were made as a function of temperature. The optical phonons require long counting times so the temperature-dependent measurements were restricted to the region near Γ where the optical phonons are most intense. It is found that the optical-phonon energies lower with temperature so that as one approaches the 2+ valence configuration, the optical-phonon energies become closer to those in SmS.[13] Thus, as the mixed-valence material enters the black phase both the optical- and acoustic-phonon energies approach those of SmS. No temperature-dependent widths were measured although these should be quite interesting especially at the (111) zone boundary.

TABLE I. Elastic constants and bulk modulus for $Sm_{0.75}Y_{0.25}S$ obtained from the low-q phonon data.

	100	200	300
C_{11}	11.76	9.78	12.19
C_{12}	−3.51	−4.09	−4.91
C_{44}	3.07	3.03	2.99
B	1.58	0.53	0.79

IV. MODEL CALCULATIONS

We have carried out several fitting calculations in order to investigate the extent to which the dispersion curves can be described by relatively simple force models. The phonon frequencies measured for NdSb, a compound which aside from its "normal" valence properties might be thought to be similar to SmS or YS, are described very well by a screened-rigid-ion model.[14] We have therefore fit our data for (Sm,Y)S to this model. The parameters in the model are the short-range force constants between Sm-S, Sm-Sm, and S-S; the two ionic charges Z_1 and Z_2; and α the range of the screening function which is assumed to change the Coulomb interaction between charges Z_1 and Z_2 from Z_1Z_2/r_{12} to $Z_1Z_2\exp(-\alpha r_{12})/r_{12}$. For $Z_1=Z_2=0$ the model obviously reduces to a standard Born–von Kármán force model with interactions extending to second nearest neighbors.

Calculations were carried out for models with general tensor forces, with axially symmetric forces and for various values of α. Except for the unusual shape of the LA[111] branch, the acoustic modes are fit very well by all of the models investigated. There was no difficulty in obtaining calculated curves with the LA[111] and LA[110] branches being lower in frequency than the corresponding transverse branches, and the fitted models reproduced the measured elastic constants quite well. The primary differences between the data and the model calculations existed in the optical mode dispersion curves. A substantially better overall fit to these modes could be achieved with a general tensor model than with an axially symmetric model. However, none of the models could provide an acceptable fit to the LO[111] branch. Also, the quality of fit, χ, did not depend very sensitively on the ionic charges or on the assumed screening distance as might be expected for a good electrical conductor such as (Sm,Y)S at room temperature. The values of the parameters deduced for two models with $\alpha a=1$, where a is the lattice parameter, are compared in Table II with each other and with the parameters reported for NdSb. A comparison of the experimental results with the general tensor model given in Table II is shown in Fig. 9.

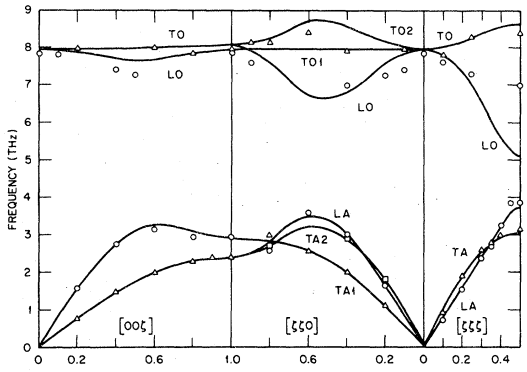

FIG. 9. Points show the phonon dispersion curve measurements at 293 K. The error bars for the measurements are about the size of the points for the acoustic branches but considerably larger for the optical branches. Details are given in Ref. 5. The solid curves are obtained from the general tensor model using parameters shown in Table II.

TABLE II. Parameters for the screened Coulomb models with $\alpha a=1$. Force constants are in units of e^2/v (v is the unit-cell volume) and the charges are in units of $|e|$.

		General tensor	Axially symmetric[a]	Axially symmetric[a]	
Sm-S	$\phi_{xx}^{(1)}$	19.5	19.8	22.8	Nd-Sb
	$\phi_{yy}^{(1)}$	3.3	2.9	−0.4	
Sm-Sm	$\phi_{xx}^{(2)}$	−0.7	0.1	2.0	Nd-Nd
	$\phi_{xy}^{(2)}$	1.2	0.6	1.7	
	$\phi_{zz}^{(2)}$	0.5	−0.5	0.3	
S-S	$\phi_{xx}^{(2)}$	0.4	−0.8	−1.5	Sb-Sb
	$\phi_{xy}^{(2)}$	−4.1	−3.2	−2.9	
	$\phi_{zz}^{(2)}$	0.4	2.4	1.4	
	Z_{Sm}	0.6	0.5	0.4	Z_{Nd}
	Z_S	−0.4	−0.5	−1.6	Z_{Sb}
	χ	1.8	2.4		

[a]For the axially symmetric model the second-neighbor constants $\phi_{xy}^{(2)}$ are constrained to be equal to $\phi_{xx}^{(2)}-\phi_{zz}^{(2)}$.

V. CONCLUSION

Neutron scattering techniques have been used to measure the phonon dispersion curves for intermediate valence $Sm_{0.75}Y_{0.25}S$ at three temperatures. Unusual features are found in both the shape of the phonon dispersion curves and the phonon widths that result from mixed-valence effects. Considerable phonon softening is found at the valence transition at 200 K. The maximum phonon widths are found in the regions of the greatest phonon softening and at the transition at 200 K. The phonon data were fit using a screened-rigid-ion model. The model roughly reproduced the general shape of the dispersion curves but fails to account for the detailed shape of the phonon anomalies, particularly for the [111] direction. The model also gives no information about the phonon widths. In appears that any model used to give a description of the phonons in $Sm_{0.75}Y_{0.25}S$ must include mixed-valence effects. Likewise any theoretical model of the mixed-valence state must not neglect the strong coupling between the phonons and valence fluctuations.

ACKNOWLEDGMENTS

The authors would like to acknowledge valuable discussions with T. Penney and N. Wakabayashi. The crystals for the experiment were provided by F. Holtzberg.

---

†Research sponsored by the Division of Materials Sciences, U.S. DOE under Contract No. W-7405-eng-26 with the Union Carbide Corporation.

[1] *Valence Instabilities and Related Narrow-Band Phenomena,* edited by R. D. Parks (Plenum, New York, 1977).

[2] For a review see C. M. Varma, Rev. Mod. Phys. 48, 219 (1976).

[3] A. Jayaraman, V. Narayanamurti, E. Bucher, and R. G. Maines, Phys. Rev. Lett. 25, 1430 (1970).

[4] S. von Molnar, T. Penny, and F. Holtzberg, J. Phys. (Paris) 37, C4-239 (1976).

[5] H. A. Mook, R. M. Nicklow, T. Penney, F. Holtzberg, and M. W. Shafer, Phys. Rev. B 18, 2925 (1978).

[6] J. L. Freeouf, D. E. Eastman, W. D. Grobman, F. Holtzberg, and J. B. Torrence, Phys. Rev. Lett. 33, 161 (1974).

[7] R. A. Pollak, F. Holtzberg, J. L. Freeouf, and D. E. Eastman, Phys. Rev. Lett. 33, 820 (1974).

[8] J. M. D. Coey, S. K. Ghatak, M. Avignon, and F. Holtzberg, Phys. Rev. B 14, 3744 (1976).

[9] H. A. Mook, T. Penney, and F. Holtzberg, J. Phys. (Paris), Colloq. 39, C6-837 (1978).

[10] R. L. Melcher, G. Guntherodt, T. Penney, and F. Holtzberg, 1975, *Ultrasonics Symposium Proceedings,* IEEE Cat. 75, CH0944-4SU, p. 616.

[11] P. D. Dernier, W. Weber, and L. D. Longinotti, Phys. Rev. B 14, 3635 (1976).

[12] G. Guntherodt, R. Merlin, A. Frey, and F. Holtzberg, International Conference on Lattice Dynamics, Paris, 1977 (unpublished).

[13] R. J. Birgeneau and S. M. Shapiro, Ref. 1, p. 49.

[14] N. Wakabayashi and A. Furrer, Phys. Rev. B 13, 4343 (1976).